Ocean Modelling 29 (2009) 147–153

Contents lists available at ScienceDirect

Ocean Modelling

journal homepage: www.elsevier.com/locate/ocemod

Short communication

Testing concepts for continuous monitoring of the meridional overturning circulation in the South Atlantic

Johanna Baehr [a,*], Adrianne Stroup [b,1], Jochem Marotzke [c]

[a] Dept. of Earth, Atmospheric, and Planetary Sciences, Massachusetts Institute of Technology, 54-1517, 77 Massachusetts Avenue, Cambridge, MA 02139, USA
[b] California Institute of Technology, Pasadena, USA
[c] Max Planck Institute for Meteorology, Bundesstrasse 53, 20146 Hamburg, Germany

ARTICLE INFO

Article history:
Received 19 June 2008
Received in revised form 17 March 2009
Accepted 21 March 2009
Available online 31 March 2009

Keywords:
Meridional Overturning circulation
Monitoring
Observing system design

ABSTRACT

We investigate if and how the monitoring strategy for the meridional overturning circulation (MOC) implemented at 26°N in the Atlantic can also be applied at a latitude in the South Atlantic. The RAPID 26°N strategy to monitor the MOC is based on continuous measurements of zonal density differences across a zonal transect, continuous measurements of the western boundary current, and additional estimates of the zonal wind stress from satellite observations. Here, we simulate a monitoring array akin to the RAPID array at 26°N in the global coupled climate ECHAM5/MPI-OM, forced with the IPCC scenario A1B. We find that the monitoring strategy can provide reliable estimates of the MOC in the South Atlantic, but the latitude needs to be carefully chosen to ensure adequate coverage of the variability arriving from both the north and the south. The limitations in the North Atlantic apply in the South Atlantic, however, we find that direct boundary current observations and bottom velocity measurements are of lesser importance for the time-mean value and the variability than in the North Atlantic. However, western boundary observations and bottom velocity measurements are crucial in capturing the vertical structure of the MOC correctly. We suggest that basin-wide MOC monitoring based on the RAPID strategy at 26°N be conducted only where boundary currents do not hit steep topography, and where bottom velocities are small.

1. Introduction

Monitoring the Atlantic meridional overturning circulation (MOC) requires the observation and understanding of both its North Atlantic and South Atlantic components. In the South Atlantic, the integrated flow of warm water is towards the equator, and the integrated flow of cold water is towards the pole (*e.g.*, Marotzke, 2000). The resulting equatorward heat transport in the South Atlantic is a unique feature of today's climate. While no new water masses are formed in the South Atlantic, it plays a crucial role in transporting and modifying remotely formed water masses with potentially important influence on both the North Atlantic MOC and heat transport. Estimates of the meridional mass and heat transports in the South Atlantic are associated with large uncertainties, and neither their time-mean values nor their variability are well understood (Ganachaud and Wunsch, 2000; Hurrell et al., 2006).

Recently, efforts have been started to launch an integrated monitoring system for heat and mass transports in the South Atlantic (Garzoli et al., 2008). In support of this effort, we assess here whether the monitoring strategy currently implemented to continuously monitor the MOC at 26°N in the Atlantic (Marotzke et al., 2002; Schiermeier, 2004; Cunningham et al., 2007; Kanzow et al., 2007) is transferable to the South Atlantic. In this note, we focus on an array based on the same combinations of components used in the 26°N array, namely, the measurements of density, zonal wind stress and boundary currents. Specifically, we test which latitude in the South Atlantic would be most suitable for MOC observation based on the RAPID 26°N monitoring strategy. Subsequently, we design the specific observing system at a potential latitude. Improving over previous observing system design studies (Hirschi et al., 2003; Baehr et al., 2004), we investigate a variety of choices for the level of no motion for this latitude.

Although this study tests the feasibility of using the currently implemented monitoring strategy at another latitude, we do not suggest that this strategy is the only imaginable MOC monitoring strategy; it is merely the only strategy that has been implemented so far. Other means of observation include satellite measurements as well as the whole variety of in situ measurements, and ultimately a synthesis of the various data sets, are essential to form a comprehensive MOC monitoring system.

* Corresponding author. Present address: Institute of Oceanography, KlimaCampus, University of Hamburg, Grindelberg 5, 20144 Hamburg, Germany. Tel.: +49 40 42838 7736.
E-mail address: johanna.baehr@zmaw.de (J. Baehr).
[1] Present address: eSolar, 130 W Union St., Pasadena, CA 91103, USA.

1463-5003/$ - see front matter © 2009 Elsevier Ltd. All rights reserved.
doi:10.1016/j.ocemod.2009.03.005

2. Data and method

2.1. Method

The RAPID 26°N monitoring strategy is based on continuous monitoring of the thermal wind, Ekman, and western boundary contributions to the MOC. Its dynamical underpinning is the thermal wind relationship, linking the zonal density gradient to the meridional flow (Marotzke, 1997; Marotzke et al., 1999; Hirschi and Marotzke, 2007). At 26°N, continuous measurements of the density field are supplemented with direct boundary current observations, ensuring coverage of the majority of the depth-averaged flow (Cunningham et al., 2007; Kanzow et al., 2007; Johns et al., 2008). Similarly to Hirschi et al. (2003) and Baehr et al. (2004), we test the behavior of the observing system by deploying it into a numerical model and mimicking the observations.

Specifically, we test the monitoring strategy by mimicking the observations of density ('density profiles'), zonal wind stress and the western boundary in the numerical model. Using these 'observations' we calculate the meridional velocities and the Ekman transport. First, for the density profiles, we subsample the model's density field over the full depth at a fixed number of longitudes. These density profiles are initially places at every zonal grid cell in the model. Subsequently the number of density profiles is reduced to resemble a feasible amount of full depth moorings. Between adjacent density profiles, we use the thermal wind relation to calculate the vertical shear. From a fixed level of no motion (initially placed at the bottom), the shear is vertically integrated to derive meridional velocities. Second, for the zonal wind stress, we zonally integrate the model's zonal wind stress across the respective latitude to obtain the Ekman transport. When mimicking western boundary measurements, we replace the meridional velocity field from thermal wind with the model's meridional velocity field. To ensure mass balance across the zonal transect, we apply a zonally constant correction to the velocity field derived from the density profiles, the zonal wind stress and – if applicable – the western boundary. From this corrected velocity field, we subsequently derive the meridional transports (the 'reconstructed MOC'). We compare this reconstructed MOC to the MOC from the model at the particular latitude considered. For MOC timeseries, we compare the vertical maximum MOC from both the reconstructed MOC and the model MOC at the particular latitude considered.

Note that we test the observing systems' ability to capture the long-term variability of the MOC by testing different designs for the density profiles. For the Ekman part, we essentially assume continuous measurements of the wind stress (from satellites) covering the entire Ekman transport and its (changes in the) variability.

2.2. Model output

The model output analyzed here stems from the coupled global climate model ECHAM5/MPI-OM (Roeckner et al., 2003; Marsland et al., 2003). ECHAM5 is realized at T63 spectral resolution (approximately 140×210 km grid spacing at mid-latitudes) with 31 vertical levels. MPI-OM is realized on an orthogonal curvilinear C-grid (Marsland et al., 2003). MPI-OM has an average horizontal resolution of about 1.5°. In the vertical, there are 40 non-equidistant z-levels, of which 20 are distributed over the top 700 m. Here, we analyze an experiment forced with observed greenhouse gas concentrations between 1860 and 2000, and with the IPCC emission scenario A1B after 2000. In the A1B scenario, greenhouse gas concentrations rise from 380 to 700 ppm between the years 2000 and 2100. Starting from year 2100, the simulation is continued for another 100 years where the levels of greenhouse gases are kept at the level of the year 2100. All simulated observations are assumed to be taken as monthly means, and all MOC reconstructions are based on those. Annual mean values are formed for the figures.

3. Results

Initially, we test at which latitudes throughout the South Atlantic the monitoring strategy implemented at 26°N is capable of capturing the main characteristics of the MOC. Subsequently, the array design is refined for one specific latitude.

3.1. MOC monitoring in the South Atlantic

The method used to establish whether the monitoring strategy implemented at 26°N allows for a reconstruction of the MOC at other latitudes, entails 'deploying' a density profile at every zonal grid cell, and placing the level of no motion at the bottom. Here, we consider both the North and the South Atlantic (Fig. 1), similarly to Sime et al. (2006), Hirschi and Marotzke (2007). Improving over Sime et al. (2006), Hirschi and Marotzke (2007) we analyze both the capability of the array to capture the interannual variability of the MOC (Fig. 1a and c), and a change in the long-term behavior of the MOC (Fig. 1b and d). Here, we will refer to changes in the MOC on decadal timescales as the long-term behavior of the MOC. Outside of regions where large currents hit steep topography (*i.e.*, south and north of 10–30°N), the interannual variability is captured well throughout the entire Atlantic (Fig. 1c). The same is true for a change in the long-term behavior of the MOC (Fig. 1d). Note that this simulation is for an array without western boundary current observations, and the reconstructed MOC improves considerably if these are taken into account (*e.g.*, at 26°N (Hirschi et al., 2003; Baehr et al., 2004)).

Focusing on the MOC at about 1000 m, the interannual variability is captured well at most latitudes. However, the time-mean value is captured only at latitudes where the boundary current does not hit steep topography, or where bottom velocities are small, or both (not shown). The time-mean value is overestimated south of about 20°S, since the thermal wind contribution overestimates the transports, which is mainly due to an underestimate of the deep western boundary current. Between 11°S and 25°S the southward boundary current increases in strength, and in turn velocities close to the boundary (as well as those near the bottom) increase. North of about 20°S, the time-mean value is underestimated. This is also true if a change in the long-term behavior of the MOC occurs.

We intercompare the MOC reconstructions at 11°S, 18°S, 25°S, and 35°S in the South Atlantic (Fig. 2, Table 1) to specifically establish a single latitude for suitable MOC monitoring. At the four different latitudes, the time-mean reconstructed MOC is smaller than the maximum MOC by 4 Sv at 11°S, but larger by respectively 1.2 Sv, 7.5 Sv, and 9.0 Sv at 18°S, 25°S, and 35°S. For the full 340 year timeseries the correlations between the maximum MOC and the reconstructed MOC exceed 0.8 for all latitudes (Table 1). However, the high correlations for the full timeseries mainly represent that the reconstructed MOC captures the change in the long-term behavior of the MOC. These high correlations do not represent whether the short-term behavior is captured at all times. When only the first 100 years of the timeseries are considered, correlations are generally lower, and exceed 0.8 only at 11°S (Table 1).

Comparisons between the standard deviation of the first 100 years and the last hundred years of the 340 year simulation, show a small increase (about 0.2 Sv) in the variability of the maximum MOC at all four latitudes. The reconstructed MOC captures this increase in variability at none of the four chosen latitudes. While at

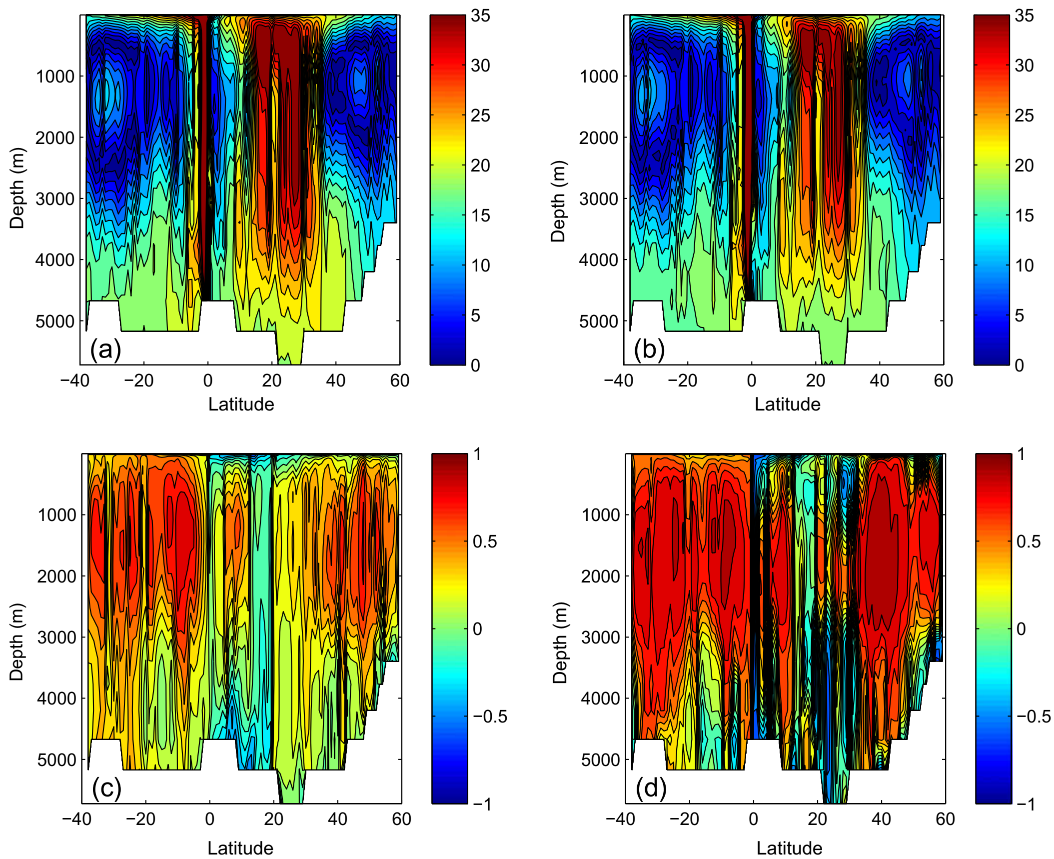

Fig. 1. Root mean square (RMS) error (top) and correlation coefficient (bottom) between the maximum MOC and the reconstructed MOC, using a density profile at each grid cell, and a level of no motion at the bottom: (a) and (c) are for the first 100 years of the realization (1860–1960) where no change in the long-term behavior of the MOC occurs. (b) and (d) are over the entire timeseries forced with the IPCC A1B scenario (340 years) where a 30% reduction occurs after about 140 years.

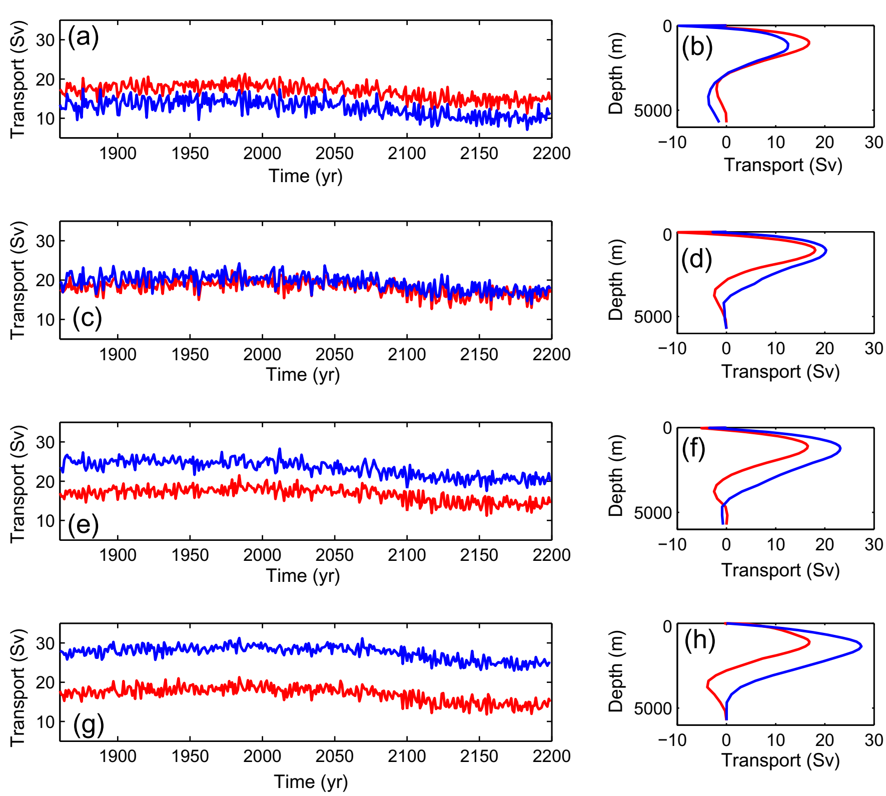

Fig. 2. Timeseries of maximum MOC (red) and reconstructed MOC (blue) based on density profiles at every longitude and level of no motion placed at the bottom. The boxes to the right show the time-mean vertical profile. 11°S (a and b), 18°S (c and d), 25°S (e and f), and 35°S (g and h). (For interpretation of the references to color in this figure legend, the reader is referred to the web version of this paper.)

Table 1
Comparison of the maximum MOC and the reconstructed MOC at different latitudes.

	11°S	18°S	25°S	35°S
Correlation (1860–1960)	0.83	0.74	0.6	0.75
Correlation (1860–2199)	0.91	0.85	0.84	0.9
Difference (time-mean in Sv)	−4.0	1.2	7.5	9.0

11°S and 18°S it overestimates the variability in the first 100 years and reproduces the variability in the last 100 years within ±0.02 Sv, at 25°S and 35°S it reproduces the variability in the first 100 years within ±0.05 Sv and underestimates the variability in the last 100 years. Note that this change in the variability of the maximum MOC is predominantly seen in the thermal wind contribution, while the change the variability of the Ekman transport is negligible.

Overall, the correlations are for both the first 100 years and the full 340 year timeseries are higher at 11°S than at the other three latitudes. Correlations are lowest at 25°S, which is close to the Confluence of the Brazil and Falkland Currents in the employed model. Differences at 18°S and 35°S are most notable in terms of the location of the Agulhas Current, which enters the basin on the east just south of 35°S, and as the Benguela Current, has nearly reached the western boundary at 18°S. Comparisons of the time-mean vertical profile of the model MOC and the reconstructed MOC (Fig. 2) indicate that the time-mean value of the reconstructed MOC at 25°S and 35°S is overestimated largely due to an underestimate of the southward flowing deep western boundary current.

We will focus on 18°S to test the design of a realistic observing system. While it is not the latitude with the highest correlation between maximum and reconstructed MOC, it shows a relatively small difference in the time-mean values of the maximum MOC and the reconstructed MOC. More importantly, it is also further south than 11°S. This is essential as the present observing system relies on thermal wind to cover the entire basin with a limited number of density profiles; non-geostrophic density fluctuations are smaller further away from the Equator, and small density fluctuations are also more enhanced through a smaller Coriolis parameter.

3.2. MOC monitoring at 18°S

The reconstructed MOC 18°S captures changes in the MOC strength and the short-term variability. So far, all our reconstructions have assumed a level of no motion at the bottom of the transect. However, the reconstructed MOC is quite sensitive to the chosen level of no motion (Fig. 3a and b). A comparison of Fig. 3a and b indicates that this sensitivity to the chosen level of no motion does not change with a change in the long-term behavior of the MOC. Differences between the first 100 years and the total timeseries are largest with respect to the long-term behavior of the MOC, which weakens both in terms of the northward transport and the southward transport. Note that for the level of no motion, a climate change signal is reconstructed at most of the different depths reasonably well, but miss considerable parts of the short-term variability (Fig. 3c). While the time-mean MOC is reconstructed accurately for a level of no motion at 1000 m, the correlation between the MOC and its reconstruction at this depth is quite small for the first hundred years (Fig. 3c). At about 4000 m, the correlation coefficient indicates a slightly improved reconstructed MOC, while the time-mean MOC is

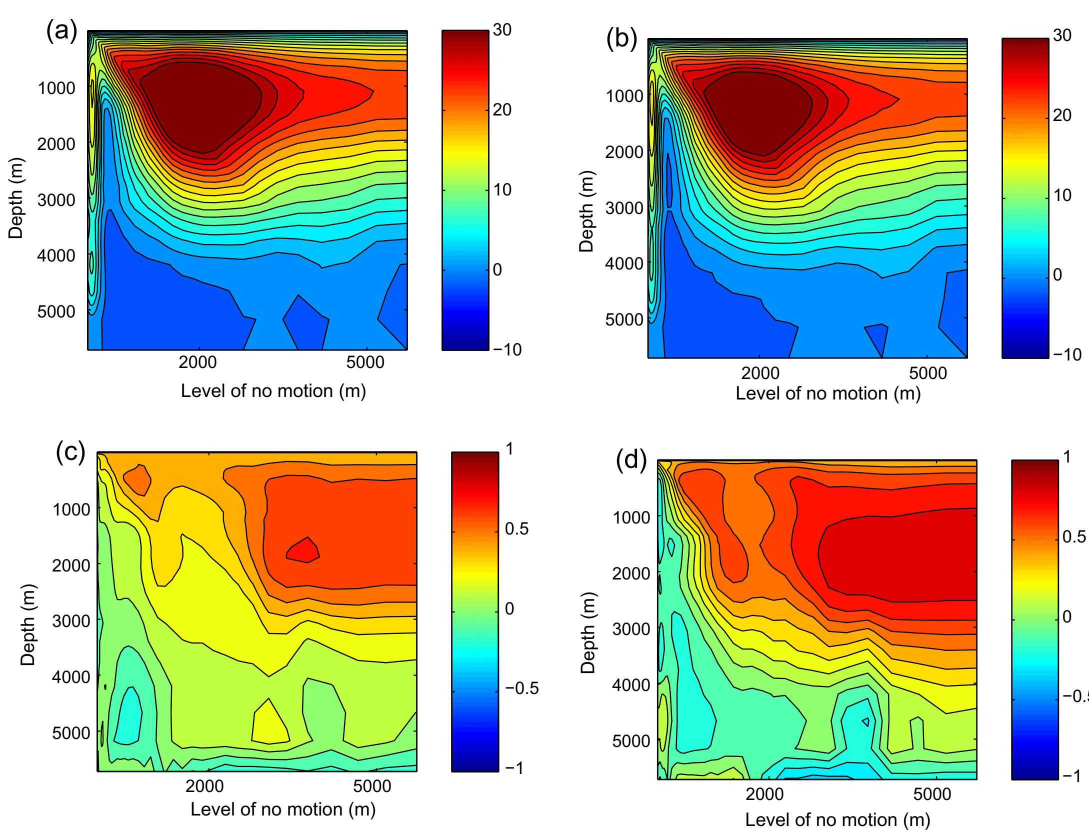

Fig. 3. (a) Time-mean vertical profile of the reconstructed MOC at 18°S for different level of no motion for the first 100 years (1860–1960) of the simulation. Abscissa indicates the level of no motion ranging from the surface to the bottom. (b) as (a) but for the entire 340 years forced with the A1B scenario. (c) Correlation coefficient between the timeseries of the maximum MOC and the reconstructed MOC both at 18°S, depending on the level of no motion, for the first 100 years of the simulation (1860–1960). (d) as (c), but for the entire 340 years forced with the A1B scenario.

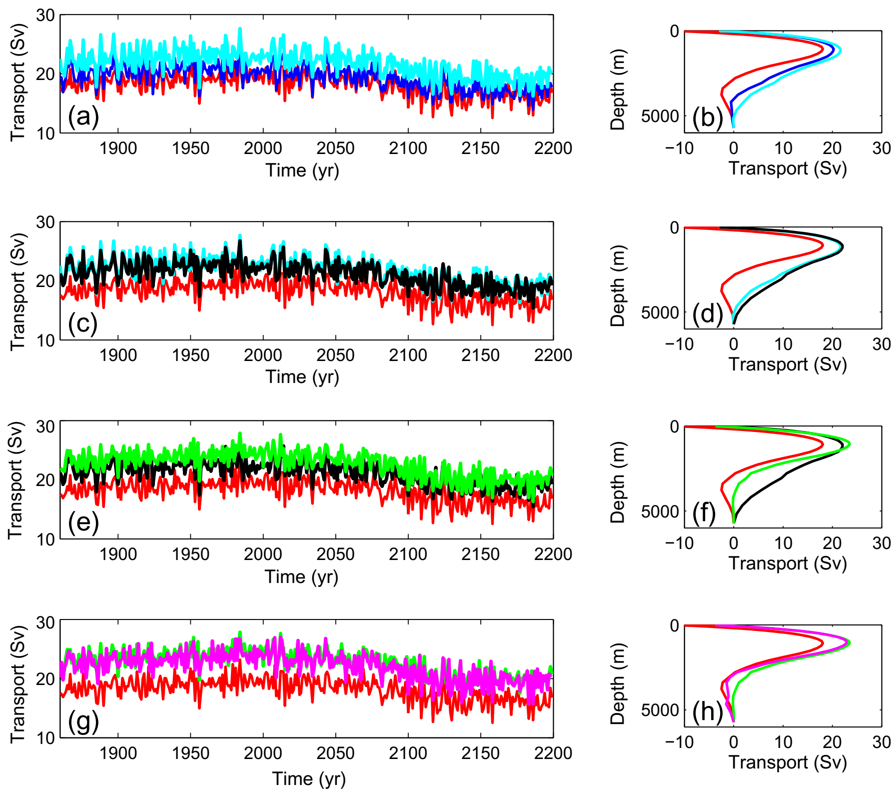

Fig. 4. 18°S, timeseries of MOC (left) and the time-mean vertical profile (right). Maximum MOC is shown in red. (a and b) Density profile at every longitude with a level of no motion at the bottom (blue) and at 3500 m (cyan). (c and d) Density profile at every longitude with a level of no motion at 3500 m (cyan), and MOC reconstruction based on 9 density profiles (black). (e and f) Nine density profiles (black), and 9 density profiles plus additional current 'observations' at the western boundary (green). (g and h) Nine density profiles plus additional current 'observations' at the western boundary (green), 9 density profiles plus additional current 'observations' at the western boundary and additional knowledge of the bottom velocities across the transect (magenta).

largely unaffected (Fig. 4a and b). Therefore, the level of no motion for 18°S is placed at about 4000 m in the following discussion.

Analyzing a latitude for potential observation primarily requires the reduction of the number of density profiles to a feasible value. When density profiles are taken at only 9 longitudes, instead of at every longitude, the quality of the reconstructed MOC is not noticeably reduced (Fig. 4c and d). Here, the density profiles are placed predominantly at the continental slopes, four at the western boundary and three at the eastern boundary. The density profiles at either side of the Mid Atlantic Ridge are of little importance. Knowledge of the western boundary current does not significantly improve the time-mean MOC reconstruction, nor does it affect the MOC variability, but it greatly improves the reconstruction of the deep flow (Fig. 4e and f). Note that extending the coverage of the western boundary either by additional density profiles or 'direct current measurements' additionally improves the variability of the reconstructed MOC due to an improved coverage of the Benguela Current variability arriving from the East. Knowledge of the bottom velocities across the entire transect results in an additional improvement of the MOC reconstruction below about 3000 m (Fig. 4g and h). In reality, both intensive boundary current observations and knowledge of the bottom velocities across the entire transect would not be feasible. Whether bottom pressure recorders could substitute for the knowledge of the bottom velocity field remains to be established.

3.3. MOC monitoring in the North and South Atlantic

Continuous MOC monitoring at 18°S would allow us to assess the MOC strength at 18°S and in the direct vicinity. Correlations between the maximum MOC at 18°S and the maximum MOC at adjacent latitudes are higher than 0.8 for the region from 13°S to 23°S approximately, when no change in the long-term behavior of the MOC occurs (Fig. 5c). Similarly, correlations between the maximum MOC at 26°N and the maximum MOC at adjacent latitudes are largest about 5° north and south of 26°N (Fig. 5a). For a change in the long-term behavior of the MOC throughout the North Atlantic and the South Atlantic, the correlations of the MOC at 18°S and 26°N are higher than 0.8 for ±20° north and south of the respective latitude (Fig. 5b and d). Therefore, temporal changes in the Atlantic MOC on the timescales of several decades could be captured by a combination of MOC observations at two distinct latitudes in the South and North Atlantic in the model. However, for interannual and decadal variability without a change in the long-term behavior of the MOC, additional observations, *e.g.*, in the North Atlantic north of about 40°N are crucial to ensure basin-wide MOC monitoring.

4. Discussion and conclusions

We examine an MOC monitoring system 'deployed' into a numerical model, and test whether the simulated array can reconstruct the MOC in the South Atlantic. We find that the quality of the reconstructed MOC is similar to what has been previously found for the North Atlantic (Hirschi et al., 2003; Baehr et al., 2004). Additionally, the model captures possible changes in the long-term behavior of the MOC at various latitudes throughout the South Atlantic. Similar to the North Atlantic, the latitudes that allow for the best reconstruction over the full water column display small bottom velocities and small depth-averaged velocities. Additionally, we find that observing the South Atlantic MOC requires capturing both the western boundary variability arriving from the

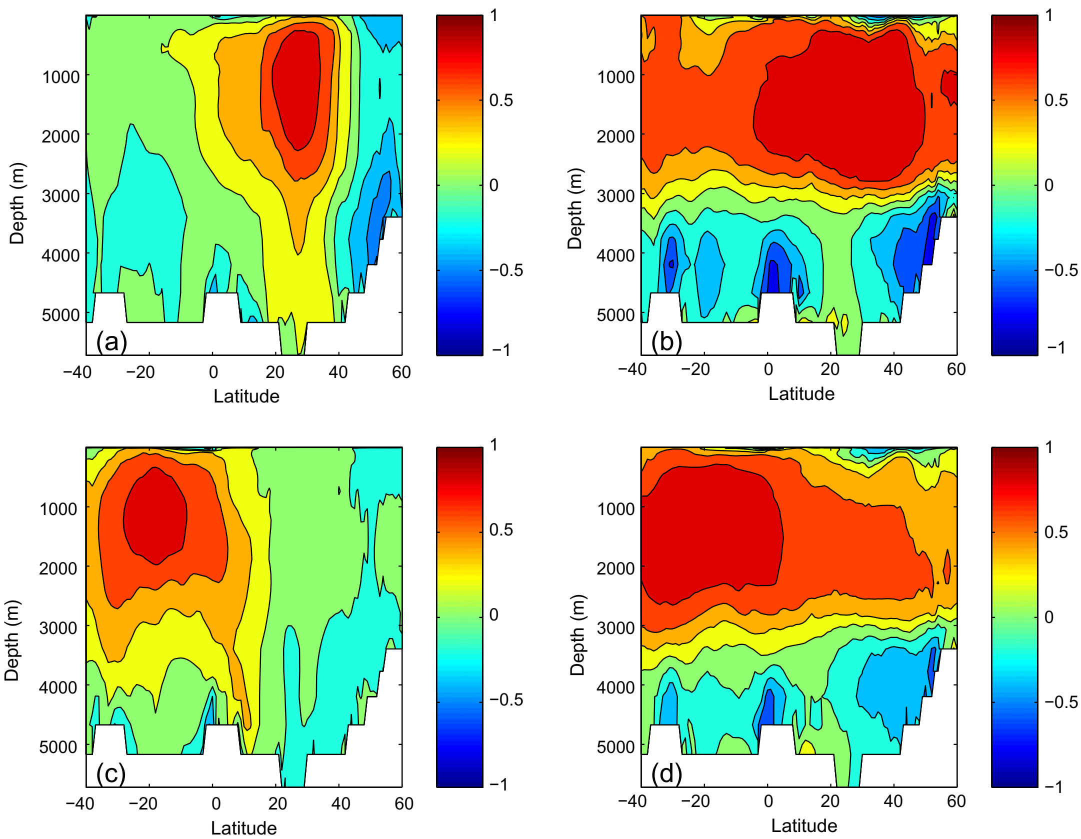

Fig. 5. (Top) Correlation coefficients between the maximum MOC at 26°N, and the Atlantic MOC for (a) the first 100 years (1860–1960), and (b) the entire 340 years (1860–2199) of the simulation. (Bottom) Correlation coefficients between the maximum MOC at 18°S, and the Atlantic MOC for the years (c) 1860–1960, and (d) 1860–2199.

North as well as the Benguela Current variability arriving from the South in agreement with Biastoch et al. (2008).

At 18°S, we find that the variability of the western boundary current can be largely captured by observing density profiles. Additional direct boundary current observations mostly improve the deep flow of the reconstructed MOC. Here, we focus on the capability of a potential array to capture both the interannual variability and potential changes in the long-term behavior of the MOC in the South Atlantic. We find that the monitoring strategy employed by the RAPID array at 26°N also provides reliable estimates in the South Atlantic within the model, for both the present day climate and a climate change scenario. However, we do not suggest that the actual choice of a potential latitude for MOC observation or the mooring placement could be based solely on the numerical model employed here. Ultimately, an analysis in a higher resolution model, with the potential restriction to shorter timescales, and a comparison to existing observations are required.

Timely detection of MOC changes will depend crucially on both the quality and quantity of the available observations. Observing the meridional transports across a zonal section is only one of many possibilities. The results presented here suggest that monitoring the MOC at 18°S could be a useful step towards a comprehensive MOC monitoring system. However, a synthesis of various data is necessary to analyze the propagation of MOC signals and, establish detection and ultimately prediction capabilities of MOC signals.

Acknowledgement

We thank Carl Wunsch for helpful comments on the manuscript. This work was supported by the Max Planck Society (J.B., J.M., A.S.), and a Monticello Scholarship by the Caltech Dean's office (AS). The computer simulations were performed at the DKRZ (Deutsches Klimarechenzentrum) in Hamburg, Germany.

References

Baehr, J., Hirschi, J., Beismann, J., Marotzke, J., 2004. Monitoring the meridional overturning circulation in the North Atlantic: a model-based array design study. Journal of Marine Research 62 (3), 283–312.

Biastoch, A., Böning, C.W., Lutjeharms, J.R.E., 2008. Agulhas leakage dynamics affects decadal variability in the Atlantic overturning circulation. Nature 456, 489–492.

Cunningham, S.A., Kanzow, T., Rayner, D., Baringer, M.O., Johns, W.E., Marotzke, J., Longworth, H.R., Grant, E.M., Hirschi, J.J.-M., Beal, L.M., Meinen, C.S., Bryden, H., 2007. Temporal variability of the Atlantic meridional overturning circulation at 26.5°N. Science 317, 935–938.

Ganachaud, A., Wunsch, C., 2000. Improved estimates of global ocean circulation, heat transport and mixing from hydrographic data. Nature 408, 453–457.

Garzoli, S.L., Piola, A., Speich, S., Baringer, M., Goni, G., Donohue, K., Meinen, C., Matano, R., 2008. A monitoring system for heat and mass transports in the South Atlantic as a component of the meridional overturning circulation. Tech. Rep. ICPO Publication Series no.125, Available from: eprints.soton.ac.uk/50121/01/125_SAMOC_report_Jan08.pdf.

Hirschi, J., Baehr, J., Marotzke, J., Stark, J., Cunningham, S., Beismann, J.-O., 2003. A monitoring design for the Atlantic meridional overturning circulation. Geophysical Research Letters 30 (7), 1413. doi:10.1029/2002GL016776.

Hirschi, J., Marotzke, J., 2007. Reconstructing the meridional overturning circulation from boundary densities and zonal wind stress. Journal of Physical Oceanography 37 (743–763).

Hurrell, J.W., Visbeck, M., Busalacchi, A., Clarke, R.A., Delworth, T.L., Dickson, R.R., Johns, W.E., Koltermann, K.P., Kushnir, Y., Marshall, D., Mauritzen, C., McCartney, M.S., Piola, A., Reason, C., Reverdin, G., Schott, F.A., Sutton, R., Wainer, I., Wright, D., 2006. Atlantic climate variability and predictability: a CLIVAR perspective. Journal of Climate 19, 5100–5121.

Johns, W.E., Beal, L.M., Baringer, M.O., Molina, J., Cunningham, S.A., Kanzow, T., Rayner, D., 2008. Variability of shallow and deep western boundary currents off the Bahamas during 2004–2005: first results from the 26N RAPID-MOC array. Journal of Physical Oceanography 38, 605–623.

Kanzow, T., Cunningham, S.A., Rayner, D., Hirschi, J.J.-M., Johns, W.E., Baringer, M.O., Bryden, H.L., Beal, L.M., Meinen, C.S., Marotzke, J., 2007. Observed flow

compensation associated with the MOC at 26.5°N in the Atlantic. Science 317, 938–941.
Marotzke, J., 1997. Boundary mixing and the dynamics of three-dimensional thermohaline circulations. Journal of Physical Oceanography 27, 1713–1728.
Marotzke, J., 2000. Abrupt climate change and thermohaline circulation: mechanisms and predictability. Proceedings of the National Academy of Sciences of the United States of America 97, 1347–1350.
Marotzke, J., Cunningham, S.A., Bryden, H.L., 2002. Monitoring the Atlantic meridional overturning circulation at 26.5°N. Proposal accepted by the Natural Environment Research Council (UK). Available from: <http://www.noc.soton.ac.uk/rapidmoc/>.
Marotzke, J., Giering, R., Zhang, K.Q., Stammer, D., Hill, C., Lee, T., 1999. Construction of the adjoint MIT ocean general circulation model and application to Atlantic heat transport sensitivity. Journal of Geophysical Research 104, 29,529–29,547.
Marsland, S.J., Haak, H., Jungclaus, J.H., Latif, M., Röske, F., 2003. The Max-Planck-Institute global ocean/sea ice model with orthogonal curvilinear coordinates. Ocean Modelling 5, 91–127.
Roeckner, E., Bäuml, G., Bonaventura, L., Brokopf, R., Esch, M., Giorgetta, M., Hagemann, S., Kirchner, I., Kornblueh, L., Manzinie, E., Rhodin, A., Schlese, U., Schulzweida, U., Tompkins, A., 2003. The atmospheric general circulation model ECHAM5, part I: model description. Tech. Rep. 349, Max Planck Institute for Meteorology.
Schiermeier, Q., 2004. Gulf Stream probed for early warnings of system failure. Nature 427, 769.
Sime, L., Stevens, D.P., Heywood, K.J., Oliver, K.I.C., 2006. A decomposition of the Atlantic meridional overturning. Journal of Physical Oceanography 36, 2253–2270.